OPEN ACCESS Freely available online

PLOS ONE

Traffic Experiment Reveals the Nature of Car-Following

Rui Jiang[1,2]*, Mao-Bin Hu[2], H. M. Zhang[3,4], Zi-You Gao[1], Bin Jia[1], Qing-Song Wu[2], Bing Wang[5], Ming Yang[5]

1 MOE Key Laboratory for Urban Transportation Complex Systems Theory and Technology, Beijing Jiaotong University, Beijing, China, **2** State Key Laboratory of Fire Science and School of Engineering Science, University of Science and Technology of China, Hefei, Anhui, China, **3** Department of Civil and Environmental Engineering, University of California Davis, Davis, California, United States of America, **4** Department of Traffic Engineering, School of Transportation Engineering, Tongji University, Shanghai, China, **5** Department of Automaton, Shanghai Jiaotong University, Shanghai, China

Abstract

As a typical self-driven many-particle system far from equilibrium, traffic flow exhibits diverse fascinating non-equilibrium phenomena, most of which are closely related to traffic flow stability and specifically the growth/dissipation pattern of disturbances. However, the traffic theories have been controversial due to a lack of precise traffic data. We have studied traffic flow from a new perspective by carrying out large-scale car-following experiment on an open road section, which overcomes the intrinsic deficiency of empirical observations. The experiment has shown clearly the nature of car-following, which runs against the traditional traffic flow theory. Simulations show that by removing the fundamental notion in the traditional car-following models and allowing the traffic state to span a two-dimensional region in velocity-spacing plane, the growth pattern of disturbances has changed qualitatively and becomes qualitatively or even quantitatively in consistent with that observed in the experiment.

Citation: Jiang R, Hu M-B, Zhang HM, Gao Z-Y, Jia B, et al. (2014) Traffic Experiment Reveals the Nature of Car-Following. PLoS ONE 9(4): e94351. doi:10.1371/journal.pone.0094351

Editor: Tobias Preis, University of Warwick, United Kingdom

Received January 11, 2014; **Accepted** March 12, 2014; **Published** April 16, 2014

Funding: RJ was supported by the National Basic Research Program of China under Grant No.2012CB725404, the Natural Science Foundation of China under Grant No. 71371175, the Research Fund for the Doctoral Program of Ministry of Education of China under Grant No. 20123402110060, and the Fundamental Research Funds for the Central Universities under Grant No.WK2320000014. MBH was supported by Natural Science Foundation of China under Grant No. 71171185. BJ was supported by the Natural Science Foundation of China under Grant No.71222101. The funders had no role in study design, data collection and analysis, decision to publish, or preparation of the manuscript.

Competing Interests: The authors have declared that no competing interests exist.

* E-mail: rjiang@ustc.edu.cn

Introduction

Vehicular traffic congestion is a serious problem all over the world, which causes huge economic loss and environmental pollution. In the last few decades, traffic flow studies have attracted wide interests of scientists from various disciplines [1-6]. This is because, on the one hand, the studies are practically important to mitigate traffic congestion, and on the other hand, traffic flow is a self-driven many-particle system far from equilibrium. The competitive, nonlinear interactions among vehicles give rise to the formation of diverse fascinating phenomena such as boundary induced phase transitions, spontaneous formation of jams, metastability, hysteresis, phase-separation, and gridlock formation [7–11]. Therefore, the study of traffic flow offers an opportunity to understand various fundamental aspects of nonequilibrium systems which are of current interest in statistical physics, such as pedestrian traffic and panics [12,13], granular flow [14], bacterial colonies [15], swarming and herding of birds and fishes [16], traveling waves in an emperor penguin huddle [17], ant trails [18], movement of molecular motors along filaments [19], dynamic arrest in glasses [20], oscillations of stock market dynamics [21], and the "bull-whip" effect of supply chain [22].

Most of the nonequilibrium phenomena of uninterrupted traffic flow on highways or expressways are closely related to traffic flow stability and specifically the growth/dissipation pattern of disturbances. However, unfortunately, there have been many controversies in traffic flow research [23–27]. Some traffic engineers believe that all traffic jams are induced by bottlenecks [23]. When traffic jams occur for no apparent reason, which is known as a phantom jam, it is only because nobody has looked far enough to find the reason. On the other hand, two decades ago, some physicists found that traffic jams can arise completely spontaneously and no bottleneck is necessary [28–30]. Under the right conditions small and local fluctuations, which happen all the time on the roads, could trigger a non-local traffic congestion that persists for hours. Recently, experimental studies on traffic flow on a circular road demonstrated that traffic jams can occur on a road without bottlenecks [31–33].

In the traditional traffic flow theory, a fundamental notion is that there is a unique relationship between the flow rate and the traffic density (or equivalently between traffic speed and vehicle spacing) under steady state conditions [34–37]. A traffic flow might be stable, metastable, or unstable. Disturbances in the metastable and unstable traffic flows could grow and develop into oscillating traffic via a subcritical Hopf bifurcation, like limit cycles generated in nonlinear autonomous systems. The traffic flow system is thus characterized as a self-excited (autocatalytic) oscillator [35]. In contrast, in the three-phase traffic theory proposed by Kerner [38–43], it is supposed that the steady state of congested traffic occupies a two-dimensional region in the flow density plane. Kerner pointed out that there are three traffic phases: free flow, synchronized flow, and wide moving jams. Usually phase transitions from free flow to synchronized flow occur firstly. At the upstream of the synchronized flow, there exists

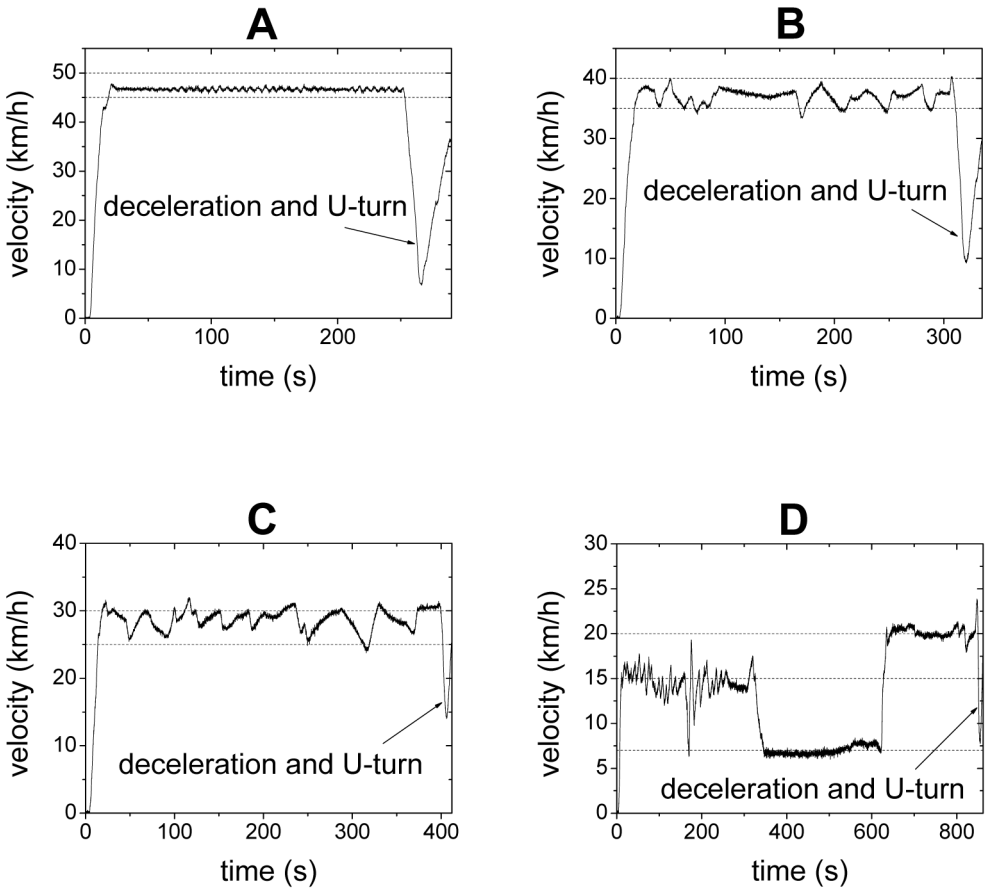

Figure 1. The velocity of the leading car. The driver of the leading car is asked to drive at 50 km/h in Panel A, 40 km/h in Panel B, 30 km/h in Panel C, firstly at 15 km/h, then to drive the car without pressing the accelerator pedal (the velocity is about 7 km/h in this case), and then to drive the car at 20 km/h in Panel D. Note that for safety reason, the actual velocity of a car is lower than that shown by the speedometer, in particular when the velocity is high. The dashed lines are guide for the eyes.
doi:10.1371/journal.pone.0094351.g001

a pinch region, in which pinch effect induces small jams. The small jams propagate towards upstream, grow, merge, and develop into wide moving jams.

The controversy between the three-phase traffic flow theory and the traditional one is still on-going, mainly due to a lack of precise traffic data [24–27]. Although there are vast amounts of empirical data collected by loop detectors, video cameras and floating cars, we are unfortunately still not able to know exactly how the traffic flow evolves even in very simple scenarios, such as in a platoon of passenger cars following each other without overtaking and led by a car moving with constant velocity. This is because, on the one hand, as claimed by Daganzo *et al.*, "no empirical studies to date describe the complete evolution of a disturbance" and thus we cannot "explain the genesis of the disturbances or the rate at which they grow" [23]. On the other hand, the empirical observations are quite site-specific and contain many confounding factors (e.g., geometry, bottleneck strength, traffic flow composition), which prevents us from forming a comprehensive understanding of traffic flow evolution.

Motivated by this problem, we conducted controlled car-following experiments to examine the traffic flow theories. Different from the previous experiments carried out on a circular road [31–33], our experiments concern a platoon of 25 passenger cars on a 3.2-km-long open road section. Since the location and velocity of each individual car have been recorded by high precision GPS devices, the complete evolution of the disturbances and their growth rate can be obtained. Moreover, in the experiments, the leading car has been asked to move with different constant speed so that various traffic flow situations can be studied, which goes beyond in-situ observations of traffic flow on roads. Therefore, general conclusions about car-following behavior are expected.

Methods

Ethics Statement

The study was approved by the institutional review board of University of Science and Technology of China. All drivers provided written informed consent.

Experimental setup

The experiment was carried out on January 19, 2013 on a 3.2 km stretch of the Chuangxin Avenue in a suburban area in Hefei City, China. There are no traffic lights on the road section. Since the road is located in a suburban area and has at least three lanes in each direction, there is no interference from other vehicles that are not part of the experiment. See Videos S1 and S2 for two typical scenarios of the experiment.

High-precision GPS devices were installed on all of the cars to record their locations and velocities every 0.1 second. The

Table 1. Sequence of the cars in the two sets of the experiment.

Sequence of Car in the platoon	Car No. in the 1st set of experiment	Car No. in the 2nd set of experiment
1	22	22
2	1	11
3	2	12
4	3	13
5	4	15
6	5	16
7	6	17
8	7	18
9	8	19
10	9	20
11	10	21
12	11	23
13	12	25
14	13	1
15	14	2
16	15	3
17	16	4
18	17	5
19	18	6
20	19	7
21	20	8
22	21	9
23	23	10
24	24	14
25	25	24

doi:10.1371/journal.pone.0094351.t001

measurement errors of the GPS devices were within $\pm$ 1 m for location and within $\pm$ 1 km/h for velocity. Once the experiment starts, the driver of the leading car is required to control the velocity of the car at certain pre-determined constant values. Other drivers in the experiment are required to drive their cars as they normally do, but overtaking is not allowed. In two of the runs, the driver of the leading car is required to firstly drive the car at 15 km/h as accurate as he can, then to drive the car without pressing the accelerator pedal (the velocity is about 7 km/h in this case), and then to drive the car at 20 km/h. In other runs, the driver of the leading car is required to accelerate the car to a pre-determined velocity and then maintain the car at the constant velocity as accurate as he can. The leading car is equipped with a cruise control system, which could be switched on when its velocity shown by the speedometer reaches 45 km/h. As a result, the fluctuation of the leading car is very small when its velocity is set at a value greater than or equal to 45 km/h. We note that for safety reason, the actual velocity of a car is lower than that shown by the speedometer, in particular when the velocity is high. See Figure 1 for the examples of the velocity of the leading car. When reaching the end of the road section, the car platoon decelerates, makes U-turn, and stops. When all the cars have stopped, a new run of the experiment begins.

Due to the length limit of the road section, we only analyze the experiment data in which the speed of the leading car is below or equal to 50 km/h. When the leading car moves with speed larger than 50 km/h, the experimental data are too limited after removing the data belonging to the start process, the deceleration and U-turn process. We have carried out two sets of experiments, in which the sequence of the cars has been changed, see Table 1.

Results

Car-following behavior

Figures 2A and 2B show two examples of the evolution of the spacing of car No. 1 (which is the second car in the platoon, see Table 1) as well as the velocities of the car and its preceding car in the first set of experiment. In Figure 2A, the car velocity is nearly constant and around 25 km/h, and the velocity difference between the car and its preceding one is always small. Before t = 174 s, the spacing fluctuates slightly around 15 m. The fundamental notion in traditional car-following theory could be correct, provided the observations before t = 174 s is the norm. However, after t = 174 s, the spacing begins to fluctuate significantly and has increased to more than 30 m, even though the traveling speed of that car remains nearly constant. Figure 2B shows that the spacing also changes significantly between 15 m and 40 m when the cars move with velocity around 41 km/h. Figures 2C-2F show some more examples of other cars, and similar results are observed.

We would like to point out fluctuations in car-following have been discussed previously, see e.g. Refs.[44–46]. For instance, by analyzing data from loop detectors as well as data from vehicle

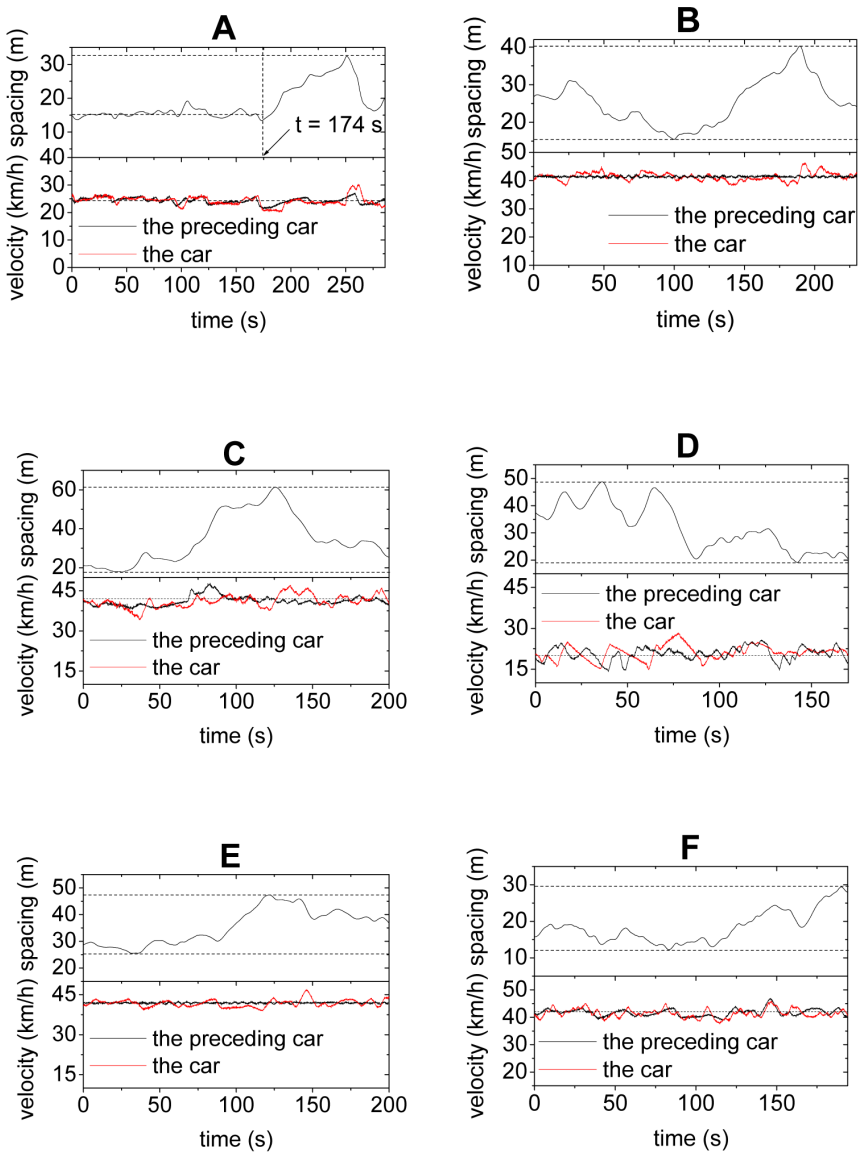

Figure 2. Evolution of velocities of a car and its preceding car and their spacing. Panels A and B show Car No. 1 in the 1st set of experiment, Panel C shows Car No. 2 in the 1st set of experiment, Panel D shows Car No. 23 in the 1st set of experiment, Panel E shows Car No. 11 in the 2nd set of experiment, Panel F shows Car No. 12 in the 2nd set of experiment. See Table 1 for the sequence of the cars in the platoon in the two sets of experiment.
doi:10.1371/journal.pone.0094351.g002

trajectories, Wagner found that the fluctuation in speed difference is around ±2 m/s, while the fluctuation in the net time headway can be as large as the mean time headway itself [44]. However, note that in the empirical data, vehicles change lane frequently. Once a vehicle or its preceding one change lane, the vehicle's spacing might change significantly. Therefore, as Wagner indicates, "unfortunately, that is no guarantee, that the data stem in fact from car-following episodes". Therefore, our experimental studies have clarified that the car-following process does lead to significant fluctuations in spacing.

This feature clearly contradicts the fundamental assumption that there is a unique relationship between vehicle speed and its spacing in traditional car-following models. Here are two possible explanations of this feature. (i) In certain range of spacing, drivers are not so sensitive to the changes in spacing when the velocity differences between cars are small. Only when the spacing is large (small) enough, will they accelerate (decelerate) to decrease (increase) the spacing. (ii) At a given velocity, drivers do not have a fixed preferred spacing. Instead they change their preferred spacing either intentionally or unintentionally from time to time in the driving process, see also Ref.[44].

Spatiotemporal features

Figures 3A–3E show some typical spatiotemporal patterns of the traffic flow. One can observe the stripes structure, which exhibits the propagation, growth, dissipation and merge of disturbances. In Figures 3A–3D, in which the leading car is not very slow, the velocity fluctuation amplitude of the cars in the rear part of the platoon has exceeded 20 km/h. In Figure 3D, in which the leading car moves with velocity around 15 km/h, some cars in the rear part of the platoon have occasionally completely stopped. In Figure 3E, in which the leading car moves very slowly with

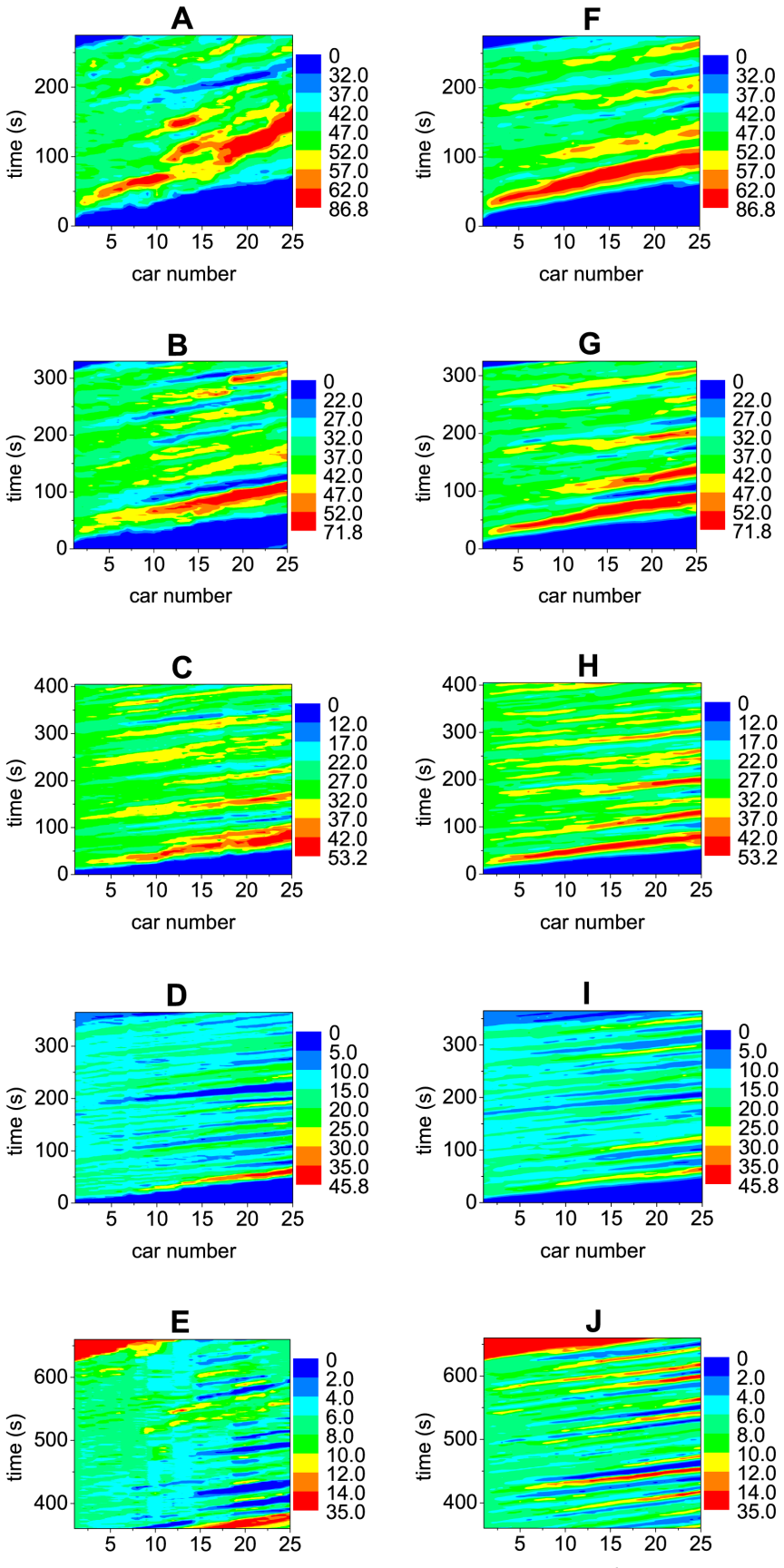
A
time (s)
car number
0
32.0
37.0
42.0
47.0
52.0
57.0
62.0
86.8
F
time (s)
car number
0
32.0
37.0
42.0
47.0
52.0
57.0
62.0
86.8
B
time (s)
car number
0
22.0
27.0
32.0
37.0
42.0
47.0
52.0
71.8
G
time (s)
car number
0
22.0
27.0
32.0
37.0
42.0
47.0
52.0
71.8
C
time (s)
car number
0
12.0
17.0
22.0
27.0
32.0
37.0
42.0
53.2
H
time (s)
car number
0
12.0
17.0
22.0
27.0
32.0
37.0
42.0
53.2
D
time (s)
car number
0
5.0
10.0
15.0
20.0
25.0
30.0
35.0
45.8
I
time (s)
car number
0
5.0
10.0
15.0
20.0
25.0
30.0
35.0
45.8
E
time (s)
0
2.0
4.0
6.0
8.0
10.0
12.0
14.0
35.0
J
time (s)
0
2.0
4.0
6.0
8.0
10.0
12.0
14.0
35.0

Figure 3. Typical spatiotemporal patterns of the platoon traffic. The car speed is shown with different colors (unit km/h) as function of time and car number. The left Panels show the experimental results and the right Panels show the simulation results of the 2D ID model. In the simulation, the velocity of the leading car is set the same as in the experiment.
doi:10.1371/journal.pone.0094351.g003

velocity around 7 km/h, the cars in the rear part of the platoon will have to completely stop from time to time.

To better understand the evolution of the disturbances, Figure 4 presents the standard deviation $\sigma_v$of the time series of the velocity of each car over all runs of the experiment, in which the leading car is asked to move with the same velocity. Note that the data belonging to the start process, the deceleration and U-turn process have been removed. One can see that when the velocity v_l of the leading car is low, σ_v increases almost linearly with car number (Figure 4A). With the increase of v_l, σ_v becomes increasing in a concave way, i.e., the curve of σ_v bends downward and the increment rate decreases (Figures 4B–4D).

Discussion

Simulations with traditional models

To study if the observed traffic features of the 25-car platoon can be reproduced with traditional car-following theories, we choose four traditional car-following models to perform traffic simulation. The details of the models and the parameters used are as follows.

- The equation of the optimal velocity (OV) model [30]:

$$\frac{dv_i}{dt}=\kappa[V(\Delta x_i)-v_i]+\xi$$

Here $\Delta x_i=x_i-1-x_i$ is the spacing of car i, which follows vehicle $i-1$. κ is sensitivity parameter. ξ is noise to represent the stochastic factors in traffic flow, which is simply assumed to be uniformly distributed random number between $-\xi_1$ and ξ_1.

The OV function used is $V(\Delta x)=11.6(\tanh(0.086(\Delta x-25))+0.913)$ [47]. The unit of length and time are meter and second, respectively. The parameters are $\kappa=1\ s^{-1}$, $\xi_1=0.2\ m/s^2$. The simulation time step $\Delta t=0.1s$

- The equation of the full velocity difference (FVD) model [48]:

$$\frac{dv_i}{dt}=\kappa[V(\Delta x_i)-v_i]+\lambda(v_i-1-v_i)+\xi$$

Here λ is another sensitivity parameter. The OV function and the noise ξ are the same as in the OV model. The parameters are $\kappa=0.32\ s^{-1}$, $\lambda=0.4\ s^{-1}$, $\xi_1=0.2\ m/s^2$. The simulation time step $\Delta t=0.1s$

- The equation of the intelligent driver (ID) model [49]:

$$\frac{dv_i}{dt}=a\left[1-\left(\frac{v_i}{v_{\max}}\right)^4-\left(\frac{s_0+v_iT+\frac{v_i(v_i-v_i-1)}{2\sqrt{ab}}}{\Delta x_i-l}\right)^2\right]+\xi$$

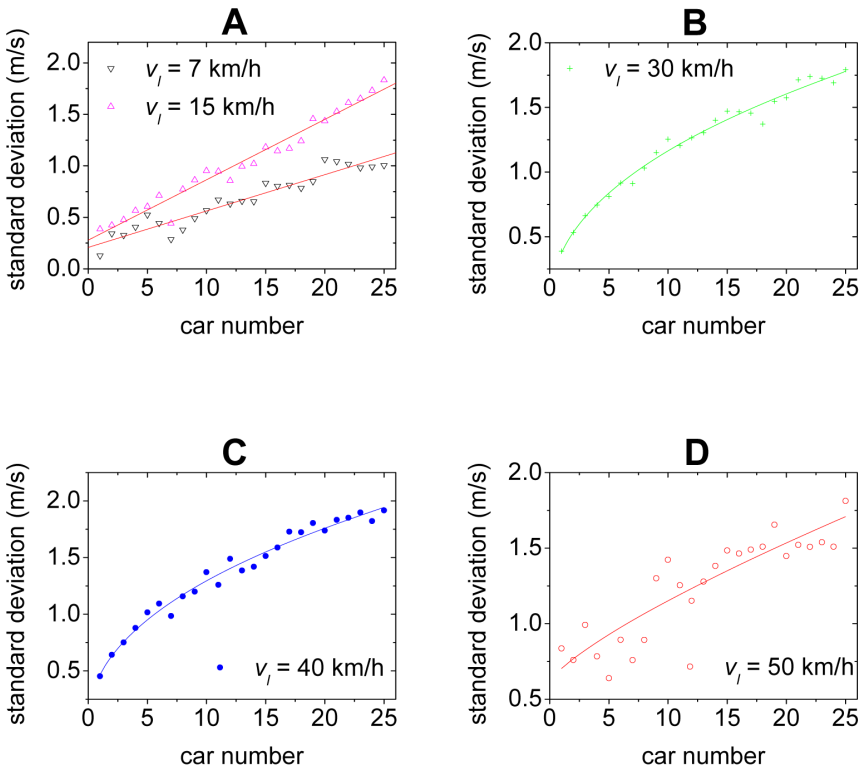

Figure 4. The standard deviation of the time series of the velocity of each car. The solid lines suggest possible curve fits.
doi:10.1371/journal.pone.0094351.g004

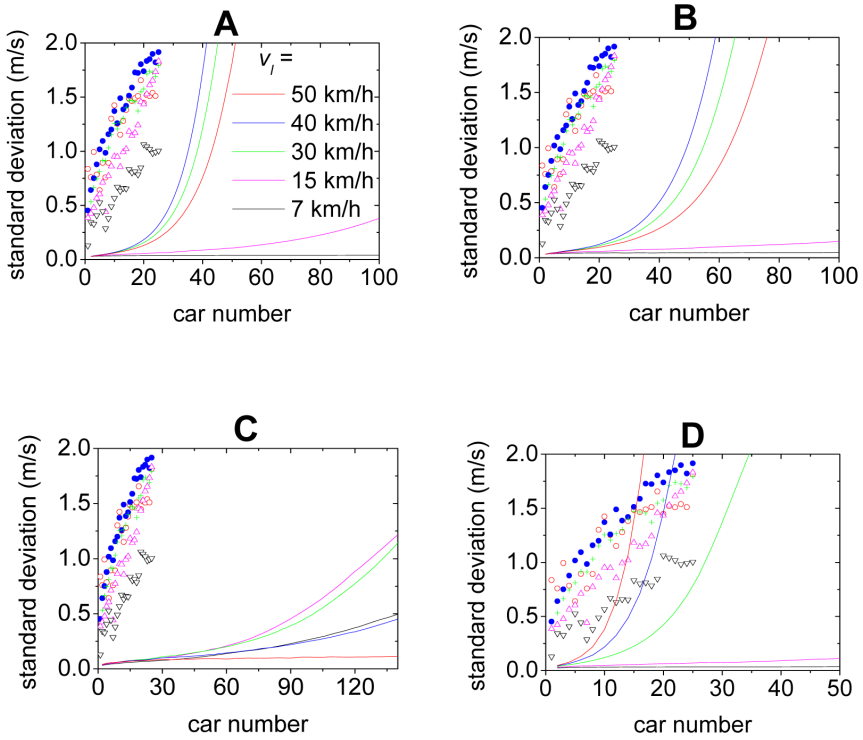

Figure 5. Simulation results (solid lines) of the standard deviation. Panel A shows the OV model, Panel B shows the FVD model, Panel C shows the ID model, Panel D shows the inertial model. The simulation results are independent of the constant acceleration of the leading car. The scatter points are from the experiment.
doi:10.1371/journal.pone.0094351.g005

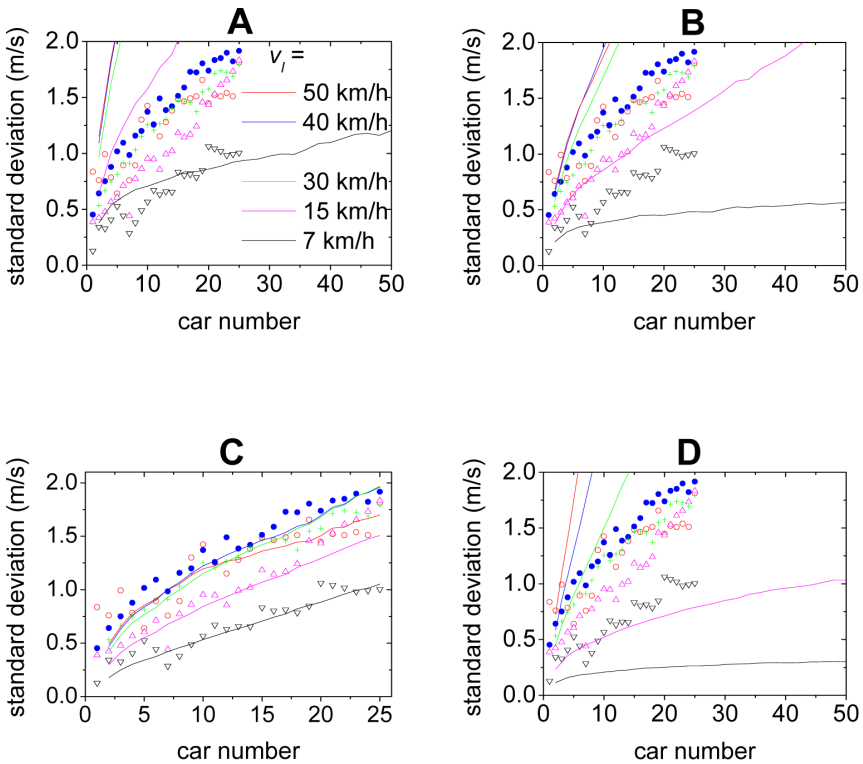

Figure 6. Simulation results (solid lines) of the standard deviation. Panel A shows the 2D OV model, Panel B shows the 2D FVD model, Panel C shows the 2D ID model, Panel D shows the 2D inertial model. The scatter points are from the experiment.
doi:10.1371/journal.pone.0094351.g006

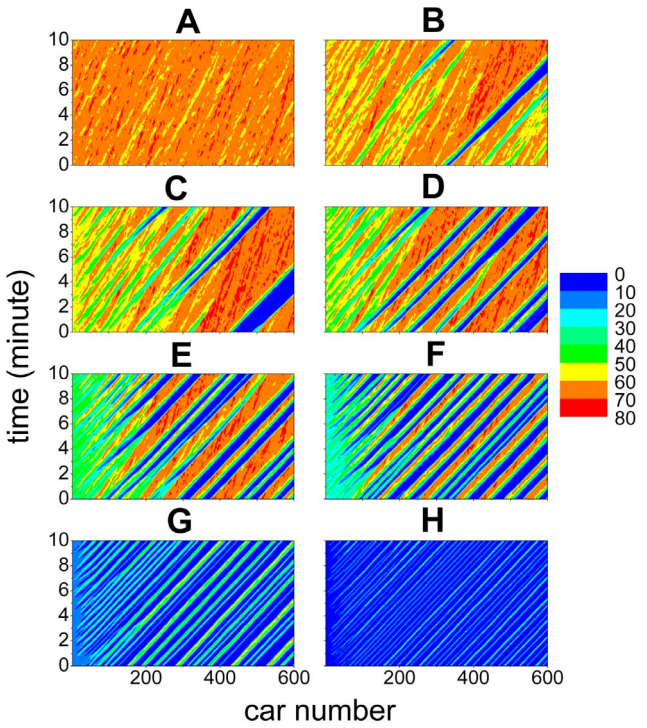

Figure 7. Simulation results of the spatiotemporal patterns in the 2D ID model. The unit of velocities is km/h. Panel A shows v_l = 65 km/h, Panel B shows v_l = 60 km/h, Panel C shows v_l = 55 km/h, Panel D shows v_l = 50 km/h, Panel E shows v_l = 40 km/h, Panel F shows v_l = 30 km/h, Panel G shows v_l = 15 km/h, Panel H shows v_l = 7 km/h.
doi:10.1371/journal.pone.0094351.g007

Here a is maximum acceleration, b is desired deceleration, T is desired time headway, s_0 is the desired gap (bumper-to-bumper distance) between two neighboring cars in jam, $v_{\max}$ is maximum velocity, l is car length, ξ is noise as before. The parameters are $v_{\max}$ = 80 km/h, T = 1.6 s, a = 0.73 m/s^2, b = 1.67 m/s^2, s_0 = 2 m, l = 5 m, ξ_1 = 0.2 m/s^2. The simulation time step $\Delta t = 0.1$s

- The equation of the inertial model [50]:

$$\frac{dv_i}{dt} = A\left(1 - \frac{v_i T + D}{\Delta x_i}\right) - \frac{Z^2(v_i - v_i - 1)}{2(\Delta x_i - D)} - kZ(v_i - v_p er) + \xi$$

Here A is a sensitivity parameter, D is the minimal distance between consecutive cars, v_{per} is the permitted velocity, k is a constant, T is the safety time gap constant, ξ is noise as before. The function Z is defined as $Z(x) = (|x| + x)/2$. The parameters are A = 5 m/s^2, D = 5 m, v_{per} = 80 km/h, k = 2 s^{-1}, T = 2 s, ξ_1 = 0.2 m/s^2. The simulation time step $\Delta t = 0.1$s

Figure 5 shows the curves of the standard deviation of the velocities of the cars. In the simulation, the leading car in an initially stopped platoon begins to accelerate with a constant acceleration until it reaches velocity v_l, then it maintains the velocity v_l. One can see that quantitatively the simulation results significantly deviate from the experimental ones. More importantly, the simulated curves increase in a convex way, which is qualitatively different from the experimental ones. Note that the observed differences between the car-following behavior of the models and empirical data has also been discussed, see e.g., Refs.[44–46] and references therein.

We would like to mention that since the velocity of a car is bounded by zero speed and the maximum speed, the standard deviation $\sigma_v$cannot grow infinitely. Thus, the curve of σ_v cannot always grow in a convex way.

Simulations with new models

We develop new models by removing the fundamental notion that there is a unique relationship between traffic speed and vehicle spacing in the steady state in the traditional models. As a result, the traffic state of a car could span a two-dimensional (2D) region in the velocity spacing plane. Thus, the new models are named as 2D models. The details of the 2D models and the parameters used are as follows.

- The 2D OV and FVD models:

We assume that the relationship between speed and spacing is determined by $V(\Delta x) = \max(11.6(\tanh(0.086(m\Delta x - 25)) + 0.913), 0)$ with a parameter m, which changes with time. For simplicity, we assume that m is a uniformly distributed random number between m_1 and m_2, and m changes in the range with rate p (i.e., in each time stepΔt in the simulation, $m \rightarrow m'$ with probability $p\Delta t$ and remains unchanged with probability 1- $p\Delta t$). In the simulations, the parameters are p = 0.15 s^{-1}, m_1 = 0.8, m_2 = 1.2. Other parameters are the same as before.

- The 2D ID model:

We suppose that the drivers do not always maintain a constant value of desired time headway T. For simplicity, we assume that T is a uniformly distributed random number between T_1 and T_2, and T changes in the range with rate p. In the simulation, the parameters are T_1 = 0.5 s, T_2 = 1.9 s, p = 0.15 s^{-1}. Other parameters are the same as before.

- The 2D inertial model:

Similar as in the 2D ID model, we assume that T is a uniformly distributed random number between T_1 and T_2, and T changes in the range with rate p. The parameters are p = 0.15 s^{-1}, T_1 = 1.6 s, and T_2 = 2.4 s. Other parameters are the same as before.

The curves of the standard deviation of the velocities of the cars in the 2D models are shown in Figure 6. One can see that although the simulation results are still quantitatively different from the experimental ones in Figures 6A, 6B, and 6D, the growth of the disturbances changes from a convex way into a concave way, which is qualitatively consistent with the experimental ones. This implies that the feature of traffic flow stability has qualitatively changed after removing the fundamental notion. As for the 2D ID model, the growth of the disturbances is not only qualitatively but also quantitatively in good agreement with the experimental ones, as shown in Figure 6C. Figures 3F–3J show the spatiotemporal patterns of the velocities simulated from the 2D ID model, in which formation of the stripes is very similar to those in the experiment.

Finally we make some predictions with the 2D ID model, which need to be validated or invalidated in future work by experimental and/or empirical data. We simulate a large platoon with 600 cars. Figure 7 shows the evolution of the velocities of the cars. One can see that when v_l is large (e.g., 65 km/h), the traffic flow is quite stable. With the decrease of v_l, the traffic flow becomes unstable and traffic jams appear more and more frequently. Moreover, the

locations where traffic jams form become closer and closer to the leading car. When v_l is low (e.g., 7 km/h and 15 km/h), high speed traffic flow cannot form between neighboring jams.

Conclusions

To summarize, we have carried out large scale car-following experiments on an open section of a road. The experimental evidence clearly runs against the traditional traffic flow theory. Simulations with traditional car-following models reproduce qualitatively different growth pattern of disturbances from the experiment. We have developed new car-following models, in which the fundamental notion in traditional traffic flow theory is removed and the traffic state of a car could span a two-dimensional region in the velocity-spacing plane. The new models are able to qualitatively or even quantitatively reproduce the growth pattern of disturbances, which implies that the feature of traffic flow stability has changed qualitatively.

We would like to note that due to the limit of road section length, the duration of the stationary state is short when the traffic speed is high (only about 2 minutes when the leading car moves with the velocity of 55 km/h). Thus, the features of high-speed traffic flow have not been revealed. Therefore, in future work, larger-scale experiments on longer road sections and with larger platoon size need to be carried out to examine the issue.

Supporting Information

Video S1 A typical scenario of the experiment.
(WMV)

Video S2 A typical scenario of the experiment.
(WMV)

Author Contributions

Conceived and designed the experiments: RJ MBH QSW . Performed the experiments: RJ MBH QSW BW MY. Analyzed the data: RJ HMZ ZYG BJ. Contributed reagents/materials/analysis tools: RJ HMZ ZYG BJ. Wrote the paper: RJ HMZ.

References

1. Chowdhury D, Santen L, Schadschneider A (2000) Statistical physics of vehicular traffic and some related systems. Phys Rep 329: 199–329.
2. Helbing D (2001) Traffic and related self-driven many-particle systems. Rev Mod Phys 73: 1067–1141.
3. Maerivoet S, De Moor B (2005) Cellular automata models of road traffic. Phys Rep 419: 1–64.
4. Nagel K, Wagner P, Woesler R (2003) Still flowing: Approaches to traffic flow and traffic jam modeling. Oper Res 51: 681–710.
5. Nagatani T (2002) The physics of traffic jams. Rep Prog Phys 65: 1331–1386.
6. Bellomo N, Dogbe C (2011) On the modeling of traffic and crowds: A survey of models, speculations, and perspectives. SIAM Rev 53: 409–463.
7. Nagel K, Schreckenberg M (1992) A cellular automaton model for freeway traffic. J Phys I (France) 2: 2221–2229.
8. Barlovic R, Santen L, Schadschneider A, Schreckenberg M (1998) Metastable states in cellular automata for traffic flow. Eur Phys J B 5: 793–800.
9. Appert C, Santen L (2001) Boundary induced phase transitions in driven lattice gases with metastable states. Phys Rev Lett 86: 2498.
10. Biham O, Middleton AA, Levine D (1992) Self-organization and a dynamical phase transition in traffic flow models. Phys. Rev. A 46: R6124–R6127.
11. Perc M (2007) Premature seizure of traffic flow due to the introduction of evolutionary games. New J Phys 9: 3.
12. Helbing D, Farkas I, Vicsek T (2000) Simulating dynamical features of escape panic. Nature 405: 487–490.
13. Moussaid M, Guillot EG, Moreau M, Fehrenbach J, Chabiron O, et al. (2012) Traffic instabilities in self-organized pedestrian crowds. PLoS Comput Biol 8: 1002442.
14. Moriyama O, Kuroiwa N, Matsushita M, Hayakawa H (1998) 4/3 law of granular particles flowing through a vertical pipe. Phys Rev Lett 80: 2833–2836.
15. Ben-Jacob E, Shochet O, Tenenbaum A, Cohen I, Czirók A, et al. (1994) Generic modeling of cooperative growth-patterns in bacterial colonies. Nature 368: 46–49.
16. Vicsek T, Czirók A, Ben-Jacob E, Cohen I, Shochet O (1995) Novel type of phase-transition in a system of self-driven particle. Phys Rev Lett 75: 1226–1229.
17. Gerum RC, Fabry B, Metzner C, Beaulieu M, Ancel A, et al. (2013) The origin of traveling waves in an emperor penguin huddle. New J Phys 15: 125022.
18. John A, Schadschneider A, Chowdhury D, Nishinari K (2009) Traffic like collective movement of ants on trails: Absence of a jammed phase. Phys Rev Lett 102: 108001.
19. Parmeggiani A, Franosch T, Frey E (2003) Phase coexistence in driven one-dimensional transport. Phys Rev Lett 90: 086601.
20. de Wijn AS, Miedema DM, Nienhuis B, Schall P (2012) Criticality in dynamic arrest: Correspondence between glasses and traffic. Phys Rev Lett 109: 228001.
21. Helbing D, Batic D, Schönhof M, Treiber M (2002) Modelling widely scattered states in 'synchronized' traffic flow and possible relevance for stock market dynamics. Physica A 303: 251–260.
22. Helbing D (2003) Modelling supply networks and business cycles as unstable transport phenomena. New J Phys 5: 90.
23. Daganzo CF, Cassidy MJ, Bertini RL (1999) Possible explanations of phase transitions in highway traffic. Transport Res A-Pol 33: 365–379.
24. Schönhof M, Helbing D (2009) Criticism of three-phase traffic theory. Transport Res B-Meth 43: 784–797.
25. Schönhof M, Helbing D (2007) Empirical features of congested traffic states and their implications for traffic modeling. Transport Sci 41: 135–166.
26. Treiber M, Kesting A, Helbing D (2010) Three-phase traffic theory and two-phase models with a fundamental diagram in the light of empirical stylized facts. Transport Res B-Meth 44: 983–1000.
27. Kerner BS (2013) Criticism of generally accepted fundamentals and methodologies of traffic and transportation theory: A brief review. Physica A 392: 5261–5282.
28. Kerner BS, Konhäuser P (1993) Cluster effect in initially homogeneous traffic flow. Phys Rev E 48: 2335–2338.
29. Kerner BS, Konhäuser P (1994) Structure and parameters of clusters in traffic flow. Phys Rev E 50: 54–83.
30. Bando M, Hasebe K, Nakayama A, Shibata A, Sugiyama Y (1995) Dynamical model of traffic congestion and numerical simulation. Phys Rev E 51: 1035–1042.
31. Sugiyama Y, Fukui M, Kikuchi M, Hasebe K, Nakayama A, et al. (2008) Traffic jams without bottlenecks - experimental evidence for the physical mechanism of the formation of a jam. New J Phys 10: 033001.
32. Nakayama A, Fukui M, Kikuchi M, Hasebe K, Nishinari K, et al. (2009) Metastability in the formation of an experimental traffic jam. New J Phys 11, 083205.
33. Tadaki S, Kikuchi M, Fukui M, Nakayama A, Nishinari K, et al. (2013) Phase transition in traffic jam experiment on a circuit. New J Phys 15: 103034.
34. Helbing D, Hennecke A, Treiber M (1999) Phase diagram of traffic states in the presence of inhomogeneities. Phys Rev Lett 82: 4360–4363.
35. Lee HY, Lee HW, Kim D (1998) Origin of synchronized traffic flow on highways and its dynamic phase transitions. Phys Rev Lett 81: 1130–1133.
36. Helbing D, Treiber M (1998) Gas-kinetic-based traffic model explaining observed hysteretic phase transition. Phys Rev Lett 81: 3042–3045.
37. Mitarai N, Nakanishi H (2000) Spatiotemporal structure of traffic flow in a system with an open boundary. Phys Rev Lett 85: 1766–1769.
38. Kerner BS, Rehborn H (1996) Experimental properties of complexity in traffic flow. Phys Rev E 53: 4275–4278.
39. Kerner BS, Rehborn H (1997) Experimental properties of phase transitions in traffic flow. Phys Rev Lett 79: 4030–4033.
40. Kerner BS (1998) Experimental features of self-organization in traffic flow. Phys Rev Lett 81: 3797–3800.
41. Kerner BS (2002) Empirical macroscopic features of spatial-temporal traffic patterns at highway bottlenecks. Phys Rev E 65: 046138.
42. Kerner BS (2004) The Physics of Traffic. Heidelberg, Springer. 682 p.
43. Kerner BS (2009) Introduction to Modern Traffic Flow Theory and Control: The Long Road to Three-Phase Traffic Theory. Berlin, Springer. 265 p.
44. Wagner P (2012) Analyzing fluctuations in car-following. Transport Res B-Meth 46: 1384–1392.
45. Wagner P (2011) A time-discrete harmonic oscillator model of human car-following. Eur Phys J B 84: 713–718.
46. Wagner P (2006) How human drivers control their vehicle. Eur Phys J B 52: 427–431.
47. Bando M, Hasebe K, Nakanishi K, Nakayama A (1998) Analysis of optimal velocity model with explicit delay. Phys Rev E 58: 5429–5435.
48. Jiang R, Wu QS, Zhu ZJ (2011) Full velocity difference model for a car-following theory. Phys Rev E 64: 017101.
49. Treiber M, Hennecke A, Helbing D (2000) Congested traffic states in empirical observations and microscopic simulations. Phys Rev E 62: 1805–1824.
50. Tomer E, Safonov L, Havlin S (2000) Presence of many stable nonhomogeneous states in an inertial car-following model. Phys Rev Lett 84: 382–385.